

1 **Supplementary Material**

2

3 **Past and Projected Weather Pattern Persistence with Associated Multi-**  
4 **Hazards in the British Isles**

5

6 Paolo De Luca<sup>1\*</sup>, Colin Harpham<sup>2</sup>, Robert L. Wilby<sup>1</sup>, John K. Hillier<sup>1</sup>, Christian L. E. Franzke<sup>3</sup>, Gregor  
7 C. Leckebusch<sup>4</sup>

8

9 <sup>1</sup>Geography and Environment, School of Social Sciences, Loughborough University, Loughborough,  
10 UK

11 <sup>2</sup>Climatic Research Unit (CRU), School of Environmental Sciences, University of East Anglia,  
12 Norwich, UK

13 <sup>3</sup>Meteorological Institute and Center for Earth System Research and Sustainability (CEN), University  
14 of Hamburg, Hamburg, Germany

15 <sup>4</sup>School of Geography Earth and Environmental Sciences, University of Birmingham, Birmingham,  
16 UK

17

18 \*Corresponding author

19 E-mail: [p.deluca@lboro.ac.uk](mailto:p.deluca@lboro.ac.uk)

20

21

22

## 23 **1. Supplementary Data and Methods**

### 24 **1.1 CMIP5, reanalyses and Lamb's catalogue**

25 The climate model output used to represent historical, future Representative Concentration Pathway  
26 8.5 (RCP8.5) and RCP4.5 projections of LWTs [1,2] originate from a multi-model sub-ensemble  
27 (MME) of 10 Atmosphere-Ocean General Circulation Models (AOGCMs) from the Coupled Model  
28 Intercomparison Project Phase 5 (CMIP5) [3]. MME output was obtained from the Earth System Grid  
29 Federation (<https://esgf-node.llnl.gov/search/cmip5/>). Per each model the historical, RCP8.5 and  
30 RCP4.5 runs of daily (12 UTC) sea-level pressure (SLP) are used to calculate daily LWTs across the  
31 BI as described above. The historical period is defined as 1980s (1971-2000). Model runs for the RCPs  
32 (2006-2100) are divided into consecutive 30-year periods covering the 2020s (2011-2040), 2050s  
33 (2041-2070) and 2080s (2071-2100). Each AOGCM was re-gridded to  $5^{\circ} \times 10^{\circ}$  (latitude  $\times$  longitude)  
34 to match the grid of the objective LWT classification [2,4]. The choice of AOGCMs was constrained  
35 by availability of daily SLP for historical, RCP8.5 and RCP4.5 runs. Table 2 lists these models along  
36 with some of their characteristics and Figures S1-S5 show results for RCP4.5.

37

38 To evaluate CMIP5 MME realism, LWTs were derived from two reanalyses [5] then compared with  
39 the 30-year historical (1980s) run of the MME. These were the 20CR [6] and NCEP [7] LWTs datasets  
40 [5], available from <https://crudata.uea.ac.uk/cru/data/lwt/>. In addition to reanalyses, we also compared  
41 the historical MME with Lamb's catalogue of subjectively defined LWTs [1,8] which ends in 1997.  
42 We evaluate the MME realism using LWTs occurring in four seasons, namely: summer (June-July-  
43 August, JJA); autumn (September-October-November, SON); winter (December-January-February,  
44 DJF); and spring (March-April-May, MAM). Seasons were assigned to the year with the first month  
45 (e.g. summer 2020 includes June 2020, July 2020 and August 2020, whilst winter 2000 includes  
46 December 2000, January 2001 and February 2001). Note that for Lamb's catalogue, DJF for the 1980s

47 has December and January for winter 1996, because the dataset ends in early February 1997. All the  
48 complete LWTs datasets used in the analyses are provided in the csv files accompanying this study.

49

## 50 **1.2 Statistical methods and analyses**

### 51 **1.2.1 2-day persistence**

52 Two-day persistence of LWTs [1,2] was derived from Markov-chain matrices of transitions between  
53 the eight main weather types defined above [9,10]. Persistence was defined as the probability that a  
54 given LWT on day( $t$ ) is followed by the same LWT on day( $t+1$ ). LWTs persistence is calculated for  
55 each AOGCM and MME mean (MMEM) for historical 1980s and 2020s, 2050s, 2080s under RCP8.5  
56 and RCP4.5. Uncertainty in persistence estimates for the CMIP5 MME 1980s was calculated by boot-  
57 strapping ( $n=1,000$ ) 30-year simulations to obtain 95% confidence intervals for significance testing.  
58 Persistence for the 2020s, 2050s and 2080s was calculated from the transition matrices. Persistence  
59 analysis was performed using the functions *markovchainFit* and *createSequenceMatrix*, from the R  
60 package ‘markovchain’ [11], respectively for historical boot-strapping and the three future periods  
61 (<https://cran.r-project.org/web/packages/markovchain/markovchain.pdf>). To evaluate the  
62 performance of the CMIP5 MME, the 20CR [6], NCEP [7], and Lamb’s subjective classification [1,8]  
63 were also used to calculate LWT persistence during the 1980s period. We also computed the CMIP5  
64 MME historical persistence for 1971-1996 (not shown here) to test the slightly shorter period covered  
65 by Lamb’s subjective catalogue. After performing a Mann-Whitney-Wilcoxon two-tailed test [12]  
66 (null hypothesis of no difference in mean persistence), between the MME 1971-1996 and MME 1980s,  
67 for A, C, W, and S LWTs within respectively summer (JJA), autumn (SON), winter (DJF) and spring  
68 (MAM), we found no statistical significance between the two periods. Therefore, we conclude that  
69 Lamb’s catalogue is equivalent to the 1980s, despite being 5 years shorter.

70

71 The seasonal persistence for each LWT, AOGCM, MMEM, 20CR, NCEP and Lamb's subjective  
72 catalogue during the 1980s and (for AOGCMs only) 2020s, 2050s and 2080s under RCP8.5 and  
73 RCP4.5 are provided in the spreadsheets accompanying this study.

74

75 The statistical significance of changes in persistence for each LWT was assessed by testing: (i)  
76 differences in the persistence of the MME between the 1980s and the 2020s, 2050s and 2080s; and ii)  
77 differences in the persistence for individual climate models in the MME. In the first case (i) we applied  
78 the Mann-Whitney-Wilcoxon two-tailed test [12] under the assumption that data are not normally  
79 distributed, with the null hypothesis of no difference in mean persistence (Tables S1-S2). The second  
80 test (ii) was performed individually for each model by checking whether persistence in the 2020s,  
81 2050s and 2080s falls outside the boot-strapped 95% confidence intervals of the 1980s (Figures 4 and  
82 S2).

83

### 84 **1.2.2 Seasonal trends**

85 Trend analysis was performed using annual series of LWT frequencies from 2006-2100 to detect both  
86 linear and non-linear changes in LWT frequencies within our CMIP5 [3] MMEM under RCP8.5 and  
87 RCP4.5 scenarios. For the sake of brevity, we only show trends for anticyclonic (A, summer JJA),  
88 cyclonic (C, autumn SON) and westerly (W, winter DJF) as indicators of impactful weather in the BI  
89 and for southerly (S, spring MAM) as this is the LWT showing most significant changes in persistence  
90 with the Mann-Whitney-Wilcoxon two-tailed test [12] (Tables S1-S2). A modified Mann-Kendall test  
91 [13], which takes into account possible autocorrelation within the time series, was applied to both  
92 RCP8.5 and RCP4.5 seasonal MMEM LWTs frequencies.

93

94 Results from the trend analysis are presented in Figures 5, S3 and Table S3 in terms of time series and  
95 Sen's slope [14] with relative statistical significance (i.e. p-value of modified Mann-Kendall test [13]).

96 Shaded bands in Figures 5 and S3 represent the 95% confidence interval of the MMEM. Sen's slope  
97 gives information about the gradient, with large Sen denoting rapid changes; the sign shows whether  
98 the trend is rising (+) or falling (-). Sen's slope values and relative statistical significance are shown  
99 in Table S3.

100

101

102

103

104

105

106

107

108

109

110

111

112

113

114

115

116

117

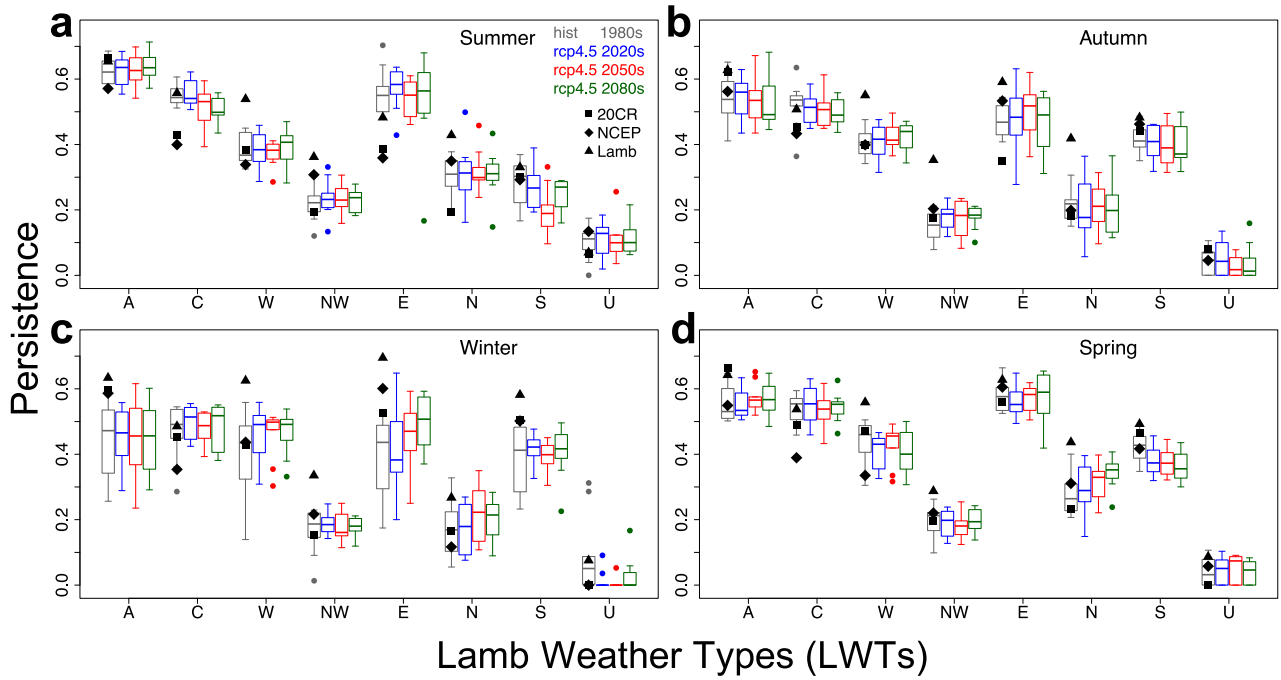
118

119

120

121 **2. Supplementary Figures**

122



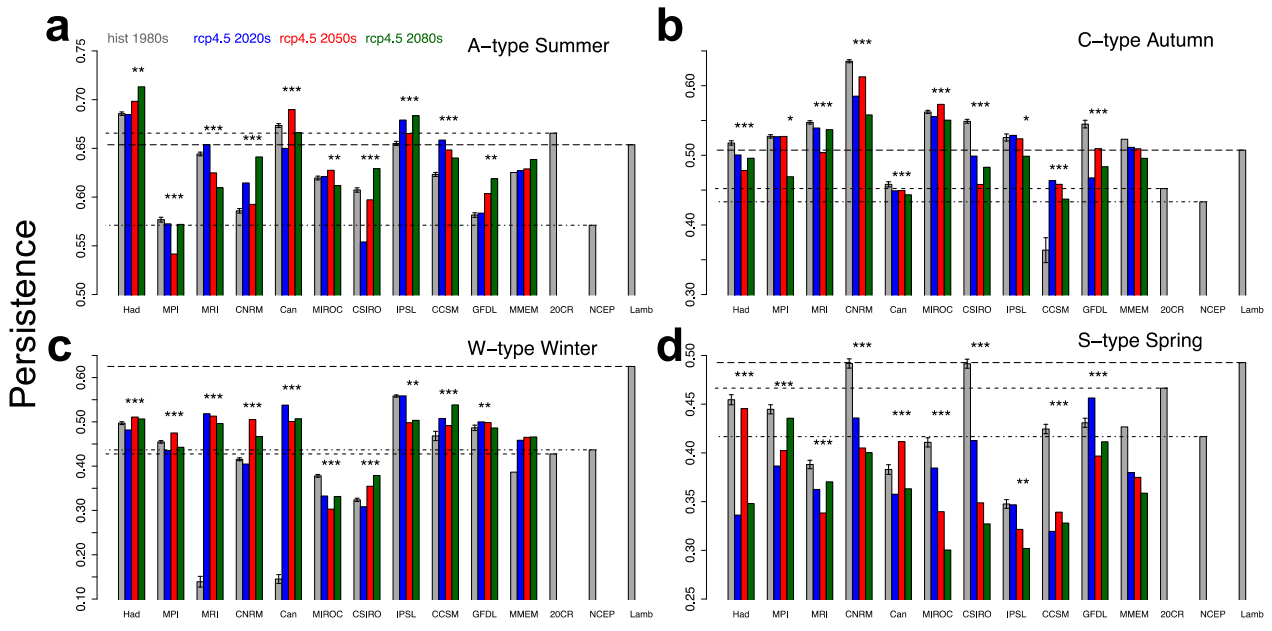
123

124 **Figure S1. As per Figure 3 but for RCP4.5.**

125

126

127



AOGCMs, MMEM, Reanalyses and Lamb

128

129 **Figure S2.** As per Figure 4 but for RCP4.5.

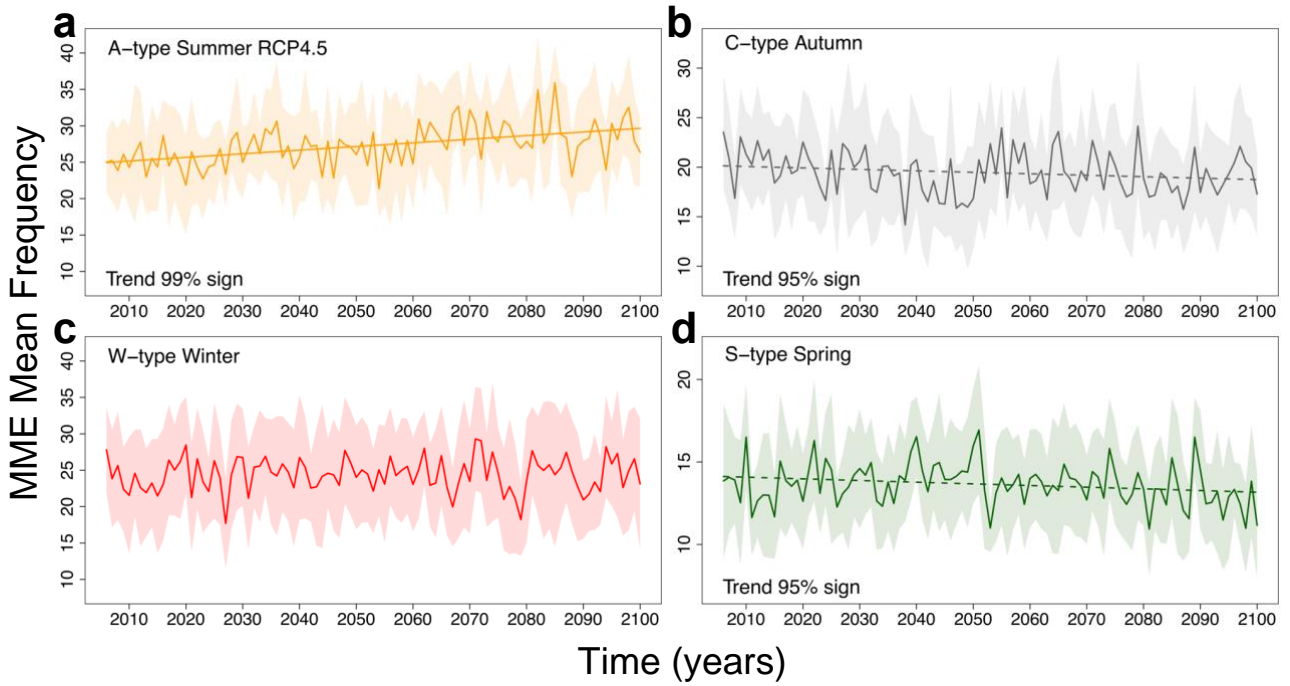
130

131

132

133

134



135

136 **Figure S3. As per Figure 5 but for RCP4.5.** Trends are statistically significant at the 1% and 5%  
 137 levels (p-value <0.01 and <0.05, modified Mann-Kendall test).

138

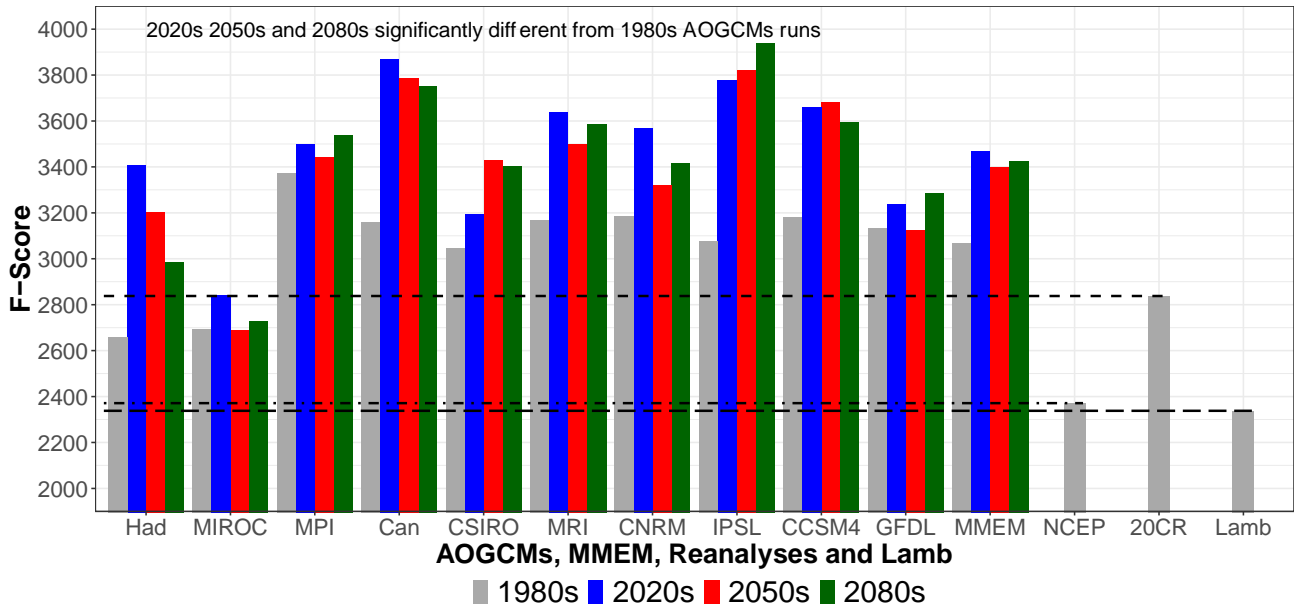
139

140

141

142

### RCP4.5 DJF



143

144 **Figure S4. As per Figure 6 but for RCP4.5.**

145

146

147

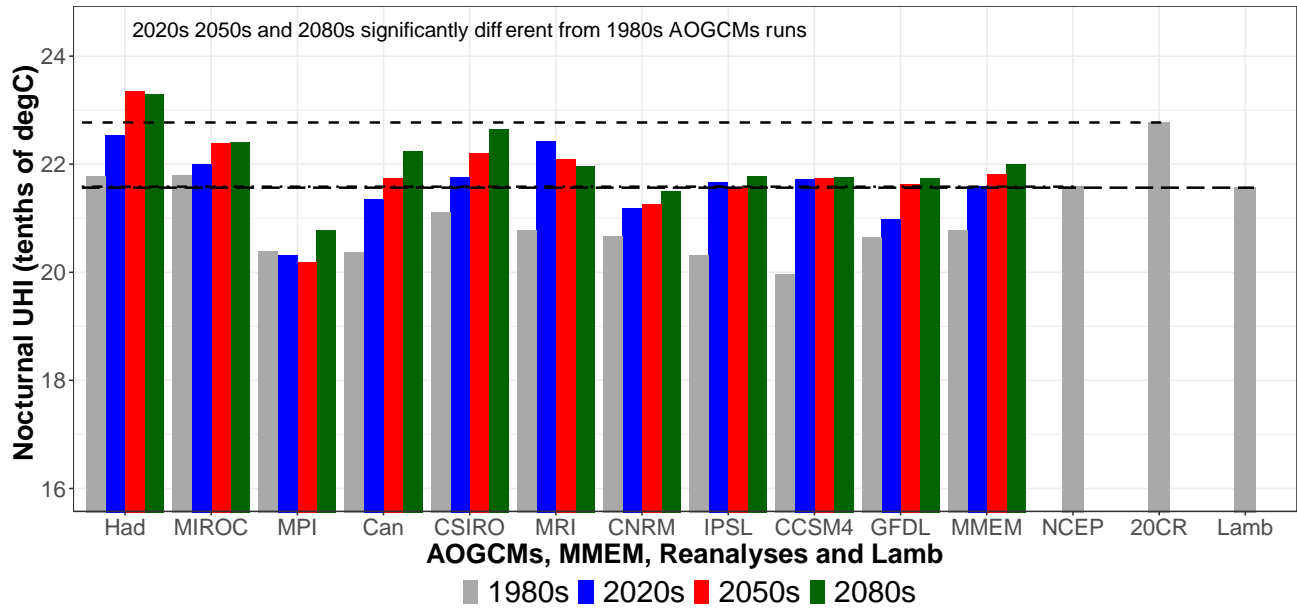
148

149

150

151

### RCP4.5 JJA



152

153 **Figure S5. As per Figure 7 but for RCP4.5.**

154

155

156

157

158

159

160

161

162

163

164

165

166

167

168

169 **3. Supplementary Tables**

170

<b>RCP8.5</b>	<b>1980s</b> <b>A</b>	<b>1980s</b> <b>C</b>	<b>1980s</b> <b>W</b>	<b>1980s</b> <b>NW</b>	<b>1980s</b> <b>E</b>	<b>1980s</b> <b>N</b>	<b>1980s</b> <b>S</b>	<b>1980s</b> <b>U</b>
<b>JJA 2020s</b>	44	60	38	47	50	38	52	62
<b>JJA 2050s</b>	42	65	40	44	54	44	68	43
<b>JJA 2080s</b>	30	<b>80</b>	51	39	<b>74</b>	34	<b>80</b>	54
<b>SON 2020s</b>	48	60	48	37	53	56	<b>76</b>	48
<b>SON 2050s</b>	54	72	39	30	53	54	<b>75</b>	42
<b>SON 2080s</b>	55	<b>74</b>	33	34	50	52	<b>78</b>	42
<b>DJF 2020s</b>	55	38	29	43	<b>24</b>	34	40	71
<b>DJF 2050s</b>	51	43	<b>24</b>	47	<b>22</b>	48	54	72
<b>DJF 2080s</b>	58	52	29	54	43	44	61	<b>90</b>
<b>MAM 2020s</b>	36	46	62	55	68	32	57	35
<b>MAM 2050s</b>	39	49	64	47	72	<b>23</b>	<b>86</b>	40
<b>MAM 2080s</b>	44	66	71	49	60	<b>19</b>	<b>88</b>	49

171

172 **Table S1. Statistical significance of LWTs persistence in the MME under RCP8.5.** Time periods  
 173 considered are the 1980s compared to the 2020s, 2050s and 2080s under RCP8.5 during all seasons:  
 174 summer JJA, autumn SON, winter DJF and spring MAM. Values shown are the W-statistic from the  
 175 Mann-Whitney-Wilcoxon two-tailed test. Statistically significant values ( $p < 0.1$ ) are shown in bold.

176

177

178

<b>RCP4.5</b>	<b>1980s A</b>	<b>1980s C</b>	<b>1980s W</b>	<b>1980s NW</b>	<b>1980s E</b>	<b>1980s N</b>	<b>1980s S</b>	<b>1980s U</b>
<b>JJA 2020s</b>	49	49	46	41	38	54	58	40
<b>JJA 2050s</b>	44	64	51	45	54	47	<b>82</b>	52
<b>JJA 2080s</b>	43	<b>82</b>	44	47	49	46	69	52
<b>SON 2020s</b>	48	60	48	30	47	58	57	50
<b>SON 2050s</b>	50	64	39	34	36	49	62	64
<b>SON 2080s</b>	60	67	36	32	49	60	65	62
<b>DJF 2020s</b>	53	41	33	47	49	44	47	<b>80</b>
<b>DJF 2050s</b>	52	54	<b>26</b>	48	36	29	54	<b>85</b>
<b>DJF 2080s</b>	50	43	31	52	<b>22</b>	34	48	<b>75</b>
<b>MAM 2020s</b>	48	44	68	54	63	38	<b>76</b>	44
<b>MAM 2050s</b>	36	56	57	64	54	31	<b>80</b>	41
<b>MAM 2080s</b>	41	51	62	50	50	<b>17</b>	<b>85</b>	50

179

180 **Table S2. The same as Table S1 but for RCP4.5.**

181

182

183

184

185

186

187

188

189

		Sen's slopes
<b>Summer JJA</b> <b>(A-type)</b>	<b>RCP8.5</b>	8.04e-02**
	<b>RCP4.5</b>	4.71e-02**
<b>Autumn SON</b> <b>(C-type)</b>	<b>RCP8.5</b>	-4.17e-02**
	<b>RCP4.5</b>	-1.71e-02*
<b>Winter DJF</b> <b>(W-type)</b>	<b>RCP8.5</b>	2.32e-02**
	<b>RCP4.5</b>	4.17e-03
<b>Spring MAM</b> <b>(S-type)</b>	<b>RCP8.5</b>	-1.88e-02**
	<b>RCP4.5</b>	-9.93e-03*

190

191 **Table S3. Sen's slopes of MMEM seasonal LWTs frequencies for RCP8.5 and RCP4.5.** The slopes  
192 are calculated using a modified Mann-Kendall trend test over the 2006-2100 period. Four LWTs are  
193 shown: anticyclonic (A) for summer JJA; cyclonic (C) autumn SON; westerly (W) winter DJF and  
194 southerly (S) spring MAM. Statistical significance is shown as \* p-value <0.05 and \*\* p-value <0.01.

195

196

197

198

199

200

201

202

203

204

## 205 **References**

- 206 [1] Lamb HH. British Isles weather types and a register of the daily sequence of circulation  
207 patterns. vol. 116. London: HMSO: 1972.
- 208 [2] Jones PD, Hulme M, Briffa KR. A comparison of Lamb circulation types with an objective  
209 classification scheme. *Int J Climatol* 1993;13:655–63. doi:10.1002/joc.3370130606.
- 210 [3] Taylor KE, Stouffer RJ, Meehl GA. An Overview of CMIP5 and the Experiment Design. *Bull*  
211 *Am Meteorol Soc* 2011;93:485–98. doi:10.1175/BAMS-D-11-00094.1.
- 212 [4] Jenkinson AF, Collison FP. An Initial Climatology of Gales over the North Sea. Synoptic  
213 Climatology Branch Memorandum No. 62, Meteorological Office, Bracknell; 1977.
- 214 [5] Jones PD, Harpham C, Briffa KR. Lamb weather types derived from reanalysis products. *Int J*  
215 *Climatol* 2013;33:1129–39. doi:10.1002/joc.3498.
- 216 [6] Compo GP, Whitaker JS, Sardeshmukh PD, Matsui N, Allan RJ, Yin X, et al. The Twentieth  
217 Century Reanalysis Project. *Q J R Meteorol Soc* 2011;137:1–28. doi:10.1002/qj.776.
- 218 [7] Kalnay E, Kanamitsu M, Kistler R, Collins W, Deaven D, Gandin L, et al. The NCEP/NCAR  
219 40-Year Reanalysis Project. *Bull Am Meteorol Soc* 1996;77:437–71.  
220 doi:[https://doi.org/10.1175/1520-0477\(1996\)077<0437:TNYRP>2.0.CO;2](https://doi.org/10.1175/1520-0477(1996)077<0437:TNYRP>2.0.CO;2).
- 221 [8] Hulme M, Barrow E. *Climate of the British Isles: present, past and future*. London: Routledge;  
222 1997.
- 223 [9] Gagniuc PA. *Markov Chains: From Theory to Implementation and Experimentation*. USA,  
224 NJ: John Wiley & Sons; 2017. doi:10.1002/9781119387596.
- 225 [10] Wilby RL. Stochastic weather type simulation for regional climate change impact assessment.  
226 *Water Resour Res* 1994;30:3395–403. doi:10.1029/94WR01840.
- 227 [11] Spedicato GA. Discrete Time Markov Chains with R. *R J* 2017;9:84–104.
- 228 [12] Mann HB, Whitney DR. On a Test of Whether one of Two Random Variables is  
229 Stochastically Larger than the Other. *Ann Math Stat* 1947;18:50–60.

230  
231  
232  
233  
234  
235

doi:10.1214/aoms/1177730491.

[13] Hamed KH, Ramachandra Rao A. A modified Mann-Kendall trend test for autocorrelated data. *J Hydrol* 1998;204:182–96. doi:[https://doi.org/10.1016/S0022-1694\(97\)00125-X](https://doi.org/10.1016/S0022-1694(97)00125-X).

[14] Sen PK. Estimates of the Regression Coefficient Based on Kendall’s Tau. *J Am Stat Assoc* 1968;63:1379–89. doi:10.1080/01621459.1968.10480934.